Visualization of Diamond Nucleation and Growth from Energetic Species

Y. Lifshitz,[1,*] X. M. Meng,[1,2] S. T. Lee,[1] R. Akhveldiany,[3] and A. Hoffman[1,3,†]

[1]*Center of Super Diamond and Advanced Films (COSDAF) and Department of Physics & Materials Science, City University Hong Kong, SAR Hong Kong, China*

[2]*Nano-organic Photoelectronic Laboratory, Technical Institute of Physics and Chemistry, Chinese Academy of Science, Beijing 100101, China*

[3]*Chemistry Department, Technion, Haifa 32000, Israel*

(Received 5 August 2003; published 27 July 2004)

The mystery of diamond nucleation by energetic species is resolved via a special deposition scheme. The evolution of the precursor material for diamond nucleation and the development of the nanodiamond crystallites are visualized by high resolution electron microscopy and other spectroscopies. The diamond precipitation and growth are explained in terms of our recently proposed mechanism [Science **297**, 1531 (2002)]: (i) precipitation of sp^3 clusters a small fraction of which are perfect diamond; (ii) growth of diamond crystallites by preferential displacement of amorphous carbon atoms leaving diamond atoms intact. This general scheme is applicable to other materials such as cubic boron nitride.

DOI: 10.1103/PhysRevLett.93.056101 PACS numbers: 81.15.–z, 68.37.–d, 68.55.–a, 81.10.–h

The unique set of properties of diamond [1–3] initiated its production by high-pressure high-temperature methods [4]. Subatmospheric medium-temperature chemical vapor deposition (CVD) techniques were further developed [1–3] to grow diamond on diamond held at ~700–800 °C. CVD diamond growth on diamond is relatively well understood [1–3]. Less so is diamond growth on nondiamond substrates which requires a nucleation stage [5]. Bias-enhanced nucleation (BEN) [6,7] is a reliable, commonly used technique developed for diamond nucleation on foreign substrates: The excited hydrocarbon-hydrogen plasma is accelerated towards the biased substrate inducing diamond nucleation by energetic particle bombardment. A subsequent nonbiased CVD stage etches away graphitic components and exposes the diamond nanocrystallites formed during BEN for further diamond growth. Very recently, we proposed a detailed diamond nucleation model [8] suggesting that fully sp^3 coordinated amorphous carbon clusters precipitate in a dense hydrogenated matrix. A very small fraction of these clusters are perfect diamond crystallites which grow under energetic atom bombardment to a size of several nm. This Letter presents a comprehensive experimental work which visualizes the nucleation and the early stages of the growth process and substantiates our proposed mechanism.

The films were deposited by CVD utilizing glow discharge for diamond nucleation [9]. The optimal nucleation conditions were [10] 10 torr, 9%CH_4:91%H_2, 500 V bias, substrate temperature 880 °C. The films were characterized by cross-sectional high resolution transmission electron microscopy (HRTEM) with its accessories (selected area electron diffraction—SAED; electron energy loss spectroscopy—EELS) in a Philips CM200 (point resolution 0.19 nm) TEM and a Gatan PEEL (parallel electron energy loss) spectrometer. The hydrogen concentration depth profile was probed by secondary ion mass spectrometry (SIMS) (Cameca 4f). The density was measured at different deposition stages using x-ray reflectivity (XRR).

Low-resolution cross-sectional TEM image of the film (Fig. 1) shows five different layers distinguished by their density, which increases with thickness (a darker layer is denser). The SAED (Fig. 2) of the first four layers is graphitic. The partial first and third graphitic rings observed are due to a preferred orientation of the graphitic basal planes in a direction perpendicular to the substrate (see the relative position of the rings with respect to the silicon spots). The SAED of the fifth layer shows diamond rings with some preferred orientation (different

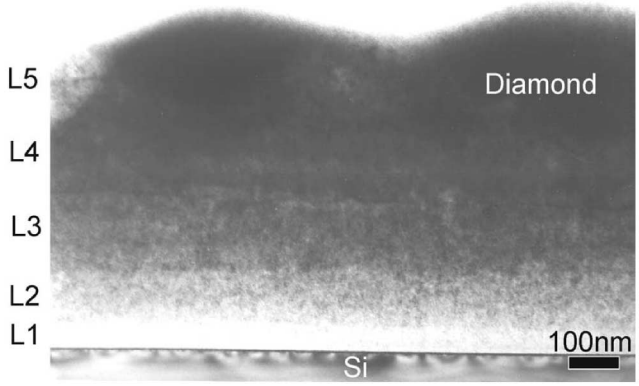

FIG. 1. Low-magnification cross-sectional TEM image of the film. A layered structure consisting of five layers with increasing density (deduced from the darkening of each layer with respect to the previous one) is observed on the Si substrate. The marking Diamond of the utmost layer denotes the nucleation layer (a diamond/graphitic carbon composite).

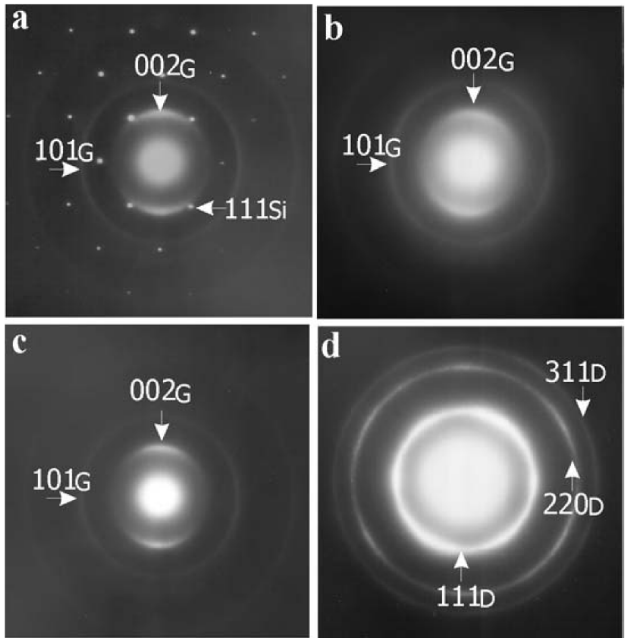

FIG. 2. Small area electron diffraction (SAED) pattern of the different layers of the film in Fig. 1. (a) Interface between Si substrate and layer 1. (b) Layer 3. (c) Layer 4. (d) Layer 5. Layers 1–4 are graphitic with an oriented structure (only partial rings). The relative orientation of the rings with respect to the Si indicates the graphitic basal planes are perpendicular to the Si surface. The rings in layer 5 are diamond rings which indicate preferred orientation (they are more intense in certain directions with symmetry similar to that of the cubic diamond lattice).

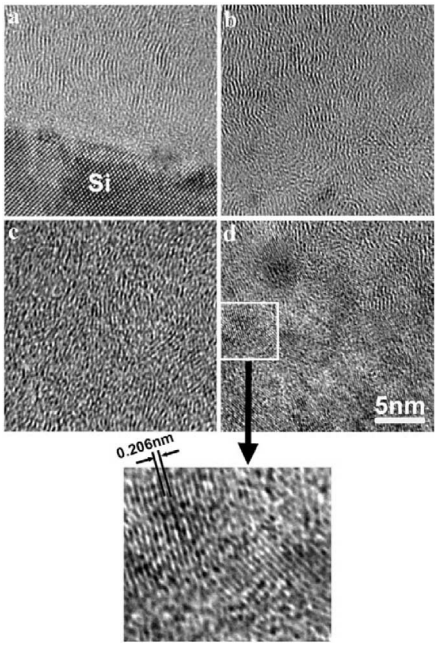

FIG. 3. Cross-sectional high-resolution TEM (HRTEM) imaging of the five layers of the film in Fig. 1. (a) Interface between Si substrate and layer 1. (b) Layer 1. (c) Layer 4. (d) Layer 5. The graphitic fringes are perpendicular to the Si surface. The films look denser as the layer develops from one to 4. Layer 5 shows 2–5 nm diamond crystallites embedded in a graphitic matrix. The marked region in *d* is enlarged to show the crystallites more clearly.

intensities in different directions) and the first graphitic ring is absent. HRTEM (Fig. 3) confirms the previous observations. The first four layers consist of oriented graphitic planes perpendicular to the substrate. The fifth layer is comprised of 2–5 nm sized crystallites with a spacing of 2.06 Å dispersed in a graphitic matrix. The EELS spectra (Fig. 4) of the first four layers exhibit a strong π^* feature (indicating a predominant sp^2 carbon component). The spectrum of the fifth layer shows the typical fine structure of cubic diamond with no π^* feature.

Figure 5 shows that the film density (XRR) increases with thickness from ~2.4–2.5 g/cm^3 in the first two layers through 2.6 to 2.8 g/cm^3 in the third and fourth layers to 3 g/cm^3 in the fifth layer. Figure 6 shows the hydrogen concentration (SIMS) which increases with thickness to reach a value of ~19 at. % [determined independently by elastic recoil detection analysis [8]].

The stages of diamond nucleation by energetic particle bombardment are [8]: (1) formation of a dense, hydrogenated amorphous carbon (*a*-C:H) layer; (2) precipitation of 100% sp^3 coordinated carbon clusters in this *a*-C:H phase via subplantation; (3) formation of a perfect diamond cluster (about one out of 10^5 to 10^6 fully sp^3 coordinated carbon clusters formed in the previous stage is perfect diamond); (4) growth of the diamond cluster by energetic species bombardment of the diamond/*a*-C:H interface. The diamond expands via preferential displacement of loosely bonded carbons leaving diamond carbon atoms intact.

The data presented can be summarized as follows: (1) the density of the layers increases with film thickness from 2.4–2.5 to 3 g/cm^3; (2) the hydrogen concentration

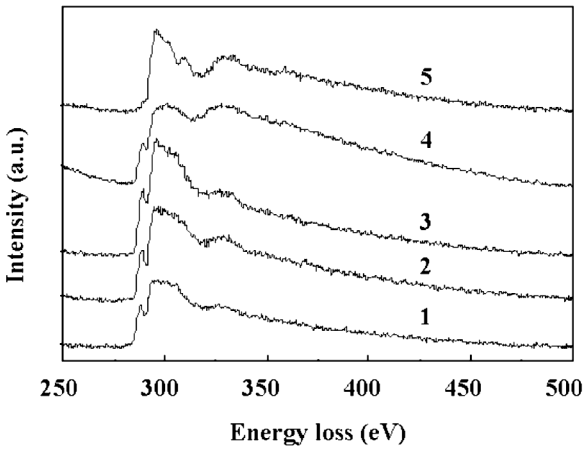

FIG. 4. Electron energy loss spectroscopy taken in the different layers in a cross-sectional sample. The first three layers are graphitic, the forth indicates an intermediate structure, and the fifth indicates a diamond structure.

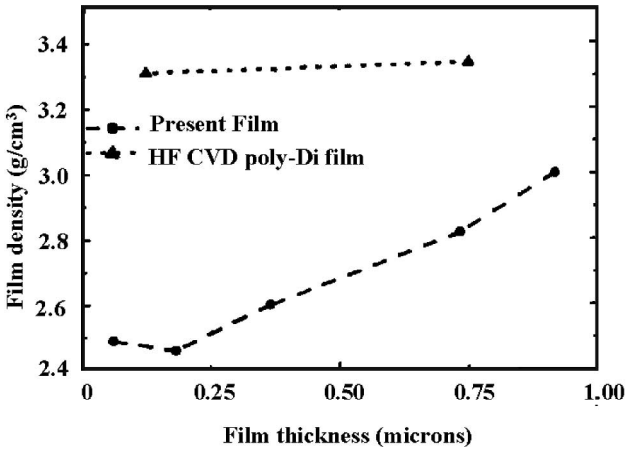

FIG. 5. X-ray reflectivity (XRR) measurements of the density of films with different thickness corresponding to the layers indicated in the cross-sectional image of Fig. 1. The density increases from 2.4–2.5 g/cm^3 in layers 1 and 2, to 2.6 in layer 3, 2.8 in layer 4, and 3 in the diamond layer. The XRR data of polycrystalline diamond films (with two different thickness values) produced by regular hot filament CVD is given for comparison

increases with thickness from 3% to 19%; (3) the first four layers consist of graphitic planes that are predominantly perpendicular to the substrate; (4) diamond precipitates in the fifth layer, which has a density of 3 g/cm^3 and a hydrogen concentration of ~19 at. %. The four first layers relate to the first nucleation stage, i.e., formation of a dense *a*-C:H phase. The formation of this dense phase is via subplantation [11,12], i.e., a shallow implantation in which the carbon and hydrogen species penetrate to subsurface layers and densification occurs by the balance between trapping (densification) and detrapping (density relaxation). The film growth by a mixture of energetic H and C particles advances through several competing processes [12]: (1) penetration and trapping of energetic atoms in subsurface layers; (2) thermal migration of atoms to the surface; (3) release of excess hydrogen; (4) chemical etching by atomic hydrogen and release of volatile hydrocarbon molecules. The growth involves simultaneous deposition and etching. The etching rate of some carbon forms (e.g., sp^2 carbon) might be larger than that of other carbon forms (e.g., diamond). More than 90% of the hydrogen atoms are not trapped in the evolving film (the H atomic concentration is ~0%–20% while the H/C ratio in the plasma for 9%CH_4/91%H_2 is 24).

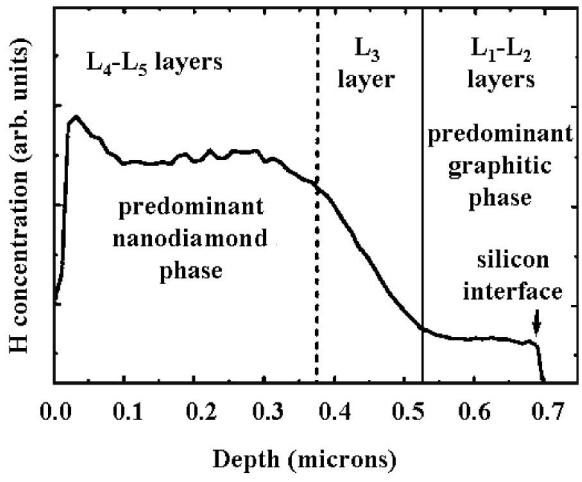

FIG. 6. SIMS depth profile of the H concentration of the film shown in Fig. 1. The hydrogen concentration is small in layers 1 and 2, increases in layer 3, and reaches a maximum in layers 4 and 5.

The first four graphitic layers are characterized by graphitic planes perpendicular to the surface, similar to films subplanted by energetic carbon ions at elevated temperatures [13,14]. The energetic bombardment induces local stress, but the elevated temperature allows modification of the evolving phase to the favorable thermodynamic configuration. The basal planes grow perpendicular to the stress (to the substrate), the most compressible way possible. The first layer is characterized by such orientation with a regular graphitic density. Once the graphitic orientation develops and the amount of amorphous material decreases (second layer), this ordered structure offers channels for the more energetic part of the hydrogen and carbon species to penetrate and be trapped between the planes. This enables a density increase and hydrogen concentration increase observed in layers 3 and 4. The density increase from 2.4–2.5 to 2.8 g/cm^3 indicates about 15%–20% carbon incorporation between the graphitic planes. A similar amount of hydrogen (15%–20% of the carbon atom density) is also trapped between the planes. The increased density and hydrogen bonding to the additional carbon atoms account for the higher trapping efficiency of hydrogen in the evolving matrix. The formation of trans-para-acetylene configurations [15] is evident from two characteristic Raman peaks around 1480 and 1140 cm^{-1} that are missing in the spectrum of the first two layers [16].

We now address the diamond nucleation in the fifth layer. Our molecular dynamics (MD) calculations show [8] that once the graphitic phase incorporates ~20% of hydrogen and carbon species and its density reaches a value of ~3 g/cm^3 100% sp^3 carbon clusters decorated by hydrogen precipitate. We suggested that a very small fraction (10^{-5}–10^{-6}) of these clusters is made of perfect diamond clusters [8]. Once they are formed they are stabilized by the boundary conditions imposed by the dense matrix. Faulty clusters can be annealed by incorporation of carbon interstitials and by hydrogen termination [8]. MD calculations by others showed [17] that graphitic edges may serve as sites for diamond nucleation, enhancing the nucleation probability. This was verified for cubic boron nitride (cBN) nucleation [18]. We failed to find evidence in our HRTEM images for a preferred nucleation of diamond on graphitic edges with the graphitic basal planes parallel to diamond (111) planes. The SAED pattern nevertheless gives some indication of

preferred orientation of diamond nanocrystals (the diffraction rings are stronger in certain directions).

We last discuss the growth of the diamond clusters to ~2–5 nm as observed in our HRTEM images. The diamond growth involves bombardment with energetic species (~100–200 eV), which mostly contain hydrogen. We suggest [8] that hydrogen atoms preferentially displace loosely bonded carbon atoms at the *a*-C:H/diamond interface, leaving the diamond atoms intact. Each loosely bonded carbon is preferentially displaced many times, and has a probability of occupying a diamond position. The diamond interface expands, consuming *a*-C:H atoms. Banhart *et al.* [19] indeed observed the expansion of diamond interface when a diamond/graphite interface was bombarded by 1.25 MeV electrons.

The present work shows that the diamond crystallites are embedded in an *a*-C/graphitic matrix. This is evident from the HRTEM images and from the near edge x-ray adsorption fine structure data [20], which show an sp^2 component covering the diamond component. In addition, exposure of diamond to pure hydrogen under similarly biased plasma conditions graphitizes all diamond forms and no diamond growth occurs in a subsequent nonbiased CVD treatment [21]. This rules out any surface nucleation process, at least in the present scheme, and leaves subplantation (bulk nucleation) as the only plausible mechanism for diamond nucleation under bombardment by energetic species.

The diamond nucleation sequence presented here resembles that of cBN [18]. In both the energetic species bombardment first forms oriented "graphitic" layers with their basal planes perpendicular to the surface. A certain layer thickness is required to facilitate nucleation of the sp^3 phase (cubic diamond or cBN). The transformation from graphitic carbon to diamond was made clear in the present work; i.e., it involves an increase of the density and the hydrogen content through incorporation of energetic C and H species between the graphitic planes. We suggest that cBN nucleation involves a similar process of densification of the "graphitic" tBN interlayer followed by precipitation of the cubic phase and its growth via preferential displacement of loosely bonded atoms of the less rigid phase. The process of (1) densification by subplantation, (2) precipitation of a dense, metastable phase, and (3) preferential growth of the metastable nuclei via bombardment seems to be general and applicable to other systems.

In summary, a comprehensive set of experimental techniques was used to characterize the nucleation process under energetic particle bombardment. The specific growth conditions provided a model system enabling the visualization of the various aspects of nucleation as: (1) subplantation growth of graphitic layers with their basal planes perpendicular to the surface; (2) a second subplantation stage in which the density increases along with an increasing hydrogen concentration; (3) precipitation of diamond nuclei in the dense *a*-C:H matrix. The present Letter provides additional insight to the diamond nucleation mechanism recently proposed [8] by us.

The work was partially supported by the Israeli Academy of Science, the Technion fund for promotion of research, the CityU SRG Grant No. 7001329, and the CityU start-up grant of Y. L. No. 9380035.

*On leave from Soreq NRC, Yavne 81800, Israel.
†Author to whom correspondence should be addressed. Electronic address: choffman@tx.technion.ac.il

[1] J. C. Angus and C. C. Hayman, Science **214**, 913 (1988).
[2] *The Physics of Diamond*, edited by A. Paoletti and A. Tucciarone, in Proceedings of the International School of Physics "Enrico Fermi," Course 135 (IOS Press, Amsterdam, 1997).
[3] Special issue on Diamond Films: Recent Developments, edited by D. M. Gruen and I. Buckley-Golder [MRS Bull. **23** (1998)].
[4] F. P. Bundy, H. T. Hall, H. M. Strong, and R. H. Wentorf, Nature (London) **176**, 51 (1955).
[5] J. Butler and H. Windischmann, MRS Bull. **23** (1998).
[6] S. Yugo, T. Kania, T. Kimura, and T. Muto, Appl. Phys. Lett. **58**, 1036 (1991).
[7] X. Jiang, C. P. Klages, R. Zachai, M. Hartweg, and H. J. Fusser, Appl. Phys. Lett. **62**, 3438 (1993).
[8] Y. Lifshitz, Th. Köhler, Th. Frauenheim, I. Gouzman, A. Hoffman, R. Q. Zhang, X. T. Zhou, and S. T. Lee, Science **297**, 1531 (2002).
[9] I. Gouzman, I. Lior, and A. Hoffman, Appl. Phys. Lett. **72**, 296 (1998).
[10] A. Hoffman, H. Heiman, H. P. Strunk, and S. H. Christiansen, J. Appl. Phys. **91**, 3336 (2002).
[11] Y. Lifshitz, S. R. Kasi, and J. W. Rabalais, Phys. Rev. Lett. **62**, 1290 (1989).
[12] Y. Lifshitz, S. R. Kasi, J. W. Rabalais, and W. Eckstein, Phys. Rev. B **41**, 10 468 (1990).
[13] J. Kulik, G. Lempert, E. Grossman, and Y. Lifshitz, *Proceedings of MRS 1999 Fall Meeting* [MRS Proc. 593, 305 (2000)].
[14] H. Y. Peng, N. Wang, Y. F. Zheng, Y. Lifshitz, J. Kulik, R. Q. Zhang C. S. Leen, and S. T. Lee, Appl. Phys. Lett. **77**, 2831 (2000).
[15] A. C. Ferrari and J. Robertson, Phys. Rev. B **63**, 121405 (2001).
[16] A. Heiman, E. Lakin, E. Zolotoyabko, and A. Hoffman, Diam. Relat. Mater. **11**, 601 (2002).
[17] W. R. Lambrecht *et al.*, Nature (London) **364**, 607 (1993).
[18] P. B. Mirkarimi, K. F. McCarty, and D. L. Medlin, Mater. Sci. Eng. **R21**, 1 (1997).
[19] F. Banhart, Rep. Prog. Phys. **62**, 1181 (1999).
[20] A. Heiman, I. Gouzman, S. H. Christiansen, H. P. Strunk, G. Comtet, L. Hellner, G. Dujardin, R. Edrei, and A. Hoffman, J. Appl. Phys. **89**, 2622 (2001).
[21] I. Bello, M. K. Fung, W. J. Zhang, K. H. Lai, Y. M. Wang, Z. F. Zhou, R. K. W. Yu, C. S. Lee, and S. T. Lee, Thin Solid Films **368**, 222 (2000).